

Corrosion Fatigue Crack Growth under Biaxial Stresses

REFERENCE Yuuki, R., Murakami, E., and Kitagawa, H., *Corrosion fatigue crack growth under biaxial stresses, Biaxial and Multiaxial Fatigue, EGF 3* (Edited by M. W. Brown and K. J. Miller), 1989, Mechanical Engineering Publications, London, pp. 285–300.

ABSTRACT Corrosion fatigue tests of a high tensile steel and a stainless steel in a 3.5 per cent NaCl solution were carried out under various in-plane biaxial stress conditions. The effects of biaxial stresses on the corrosion fatigue crack growth properties were investigated and compared with in-air data.

It is found that an effect of biaxial stresses occurs in the NaCl solution and the critical region where the effect exists coincides with that in air. However, the order of the data set for biaxial stress conditions is different in NaCl from that in air and there is also a difference between the free corrosion condition and the cathodic condition.

Introduction

A lot of fatigue crack growth data in seawater have been reported, e.g., reference (1), in order to evaluate the fatigue life, or the integrity, of offshore structures from linear elastic fracture mechanics (LEFM) analyses. However, most of the data is from simple fracture mechanics specimens subjected to uniaxial loading. No data in seawater under biaxial loadings could be found.

Recently it has been shown that fatigue crack growth in air (2)–(9) and also at elevated temperature (10) is affected by the biaxial stress state. In a previous paper (9), a significant effect of biaxial stress on fatigue crack growth in air appears even if the stress level is only about 0.4 of the yield stress when a crack is relatively small. The authors also described a critical region for which the effect of biaxial stresses on fatigue crack growth occurred in an air environment. It therefore seems important to study the effect of biaxial stresses on corrosion fatigue crack growth in seawater, especially since most offshore structures suffer biaxial and multiaxial loadings.

In this study, corrosion fatigue tests of a high tensile steel (WT60) and a stainless steel (SUS304) in a 3.5 per cent NaCl solution were carried out under various in-plane biaxial stress conditions. The effects of biaxial stresses on corrosion fatigue crack growth were investigated, and compared with those in

* Institute of Industrial Science, University of Tokyo, 7-22-1 Roppongi, Minato-ku, Tokyo, Japan.

† Kure Research Laboratory, Babcock-Hitachi Corporation, 3-36 Takara-machi, Kure, Hiroshima, Japan.

‡ Faculty of Engineering, Yokohama National University, 156 Totuwadai, Hodogaya-ku, Yokohama, Japan.

air. The applicability and the limit of applicability of LEFM to corrosion fatigue crack growth are discussed. It is expected that the effect of biaxial stresses will be different from that in air because of the interaction of environment effects such as hydrogen embrittlement and corrosion dissolution.

Notation

a	Half length of a crack
λ	Biaxial stress ratio ($=\sigma_T/\sigma_L$)
da/dN	Fatigue crack growth rate
E	Potential (Ag/AgCl)
F_I	Normalized stress intensity
f	Loading frequency
K_I	Stress intensity factor
ΔK_I	Stress intensity factor range
R_K	Stress ratio defined by K_{Imin}/K_{Imax}
U	Crack opening ratio ($=K_{max} - K_{op}/\Delta K$)
$\sigma_{y_0}, \sigma_{x_0}$	Nominal stresses applied to the gripped parts of the specimen in the y direction and the x direction, respectively
σ_L, σ_T	Stresses at the centre of the specimen without a crack
σ_{ys}	Uniaxial yield strength
ϕ	Phase difference between the load axes

The biaxial fatigue test

Fatigue tests have been performed on a high-cycle biaxial fatigue testing machine (8)(9). This machine has four electric hydraulic servo actuators and load cells, arranged perpendicular to each other on a horizontal plane in a rigid circular frame. The machine can control, with high accuracy, the mean and the amplitude of loads for both axes, as well as the phase difference, ϕ , between them. Cruciform flat specimens were used as shown in Fig. 1. A fatigue pre-crack was developed under uniaxial loading until the total crack length reached 6 mm. The high tensile steel (WT60) had a thickness of 4.5 mm and the type 304 austenitic stainless steel (SUS304) a thickness of 5 mm. The mechanical properties and chemical compositions are shown in Table 1.

The stress intensity factors for a centre crack in a cruciform specimen are calculated from the following equation; see also (9)

$$K_I = F_{Iy}\sigma_{y_0}\sqrt{\pi a} + F_{Ix}\sigma_{x_0}\sqrt{\pi a} \quad (1)$$

$$F_{Iy} = 1.4890 - 0.0077(a/L) + 0.2713(a/L)^2 - 0.0184(a/L)^3 \quad (2)$$

$$F_{Ix} = -0.3227 + 0.0062(a/L) - 0.0114(a/L)^2 + 0.0547(a/L)^3 \quad (3)$$

Where L for the current specimen is 17 mm (see Fig. 1), and σ_{y_0} and σ_{x_0} are nominal stresses applied to the gripped parts of the specimen. The values of F_{Iy} and F_{Ix} are correction factors deduced by a modified mapping collocation method.

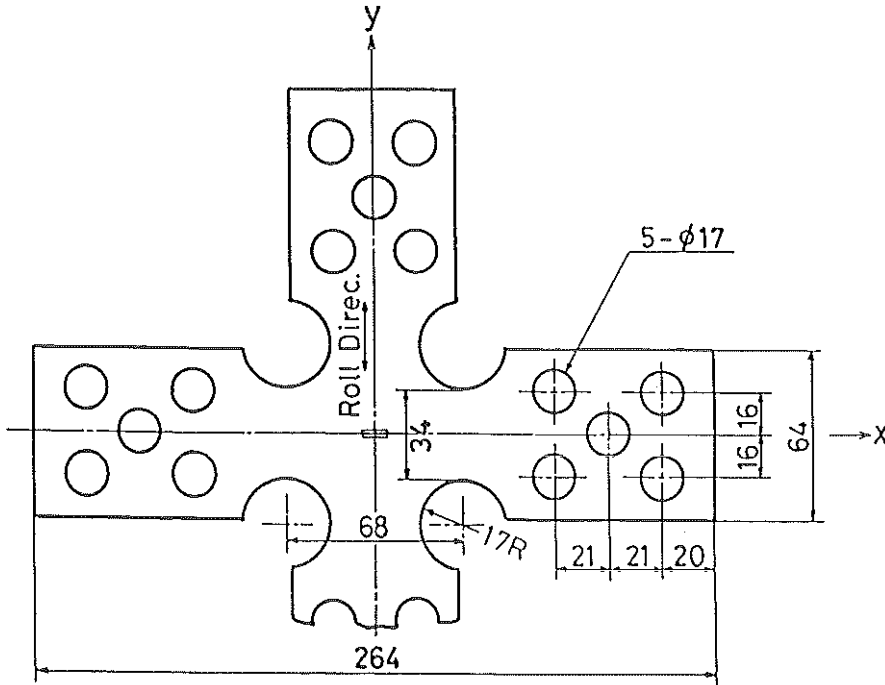


Fig 1 Cruciform specimen geometry (all dimensions in mm)

From the results of FEM analysis, the stress σ_L in the y direction and σ_T in the x direction at the centre of specimen without a crack can be represented as follows (Fig. 2)

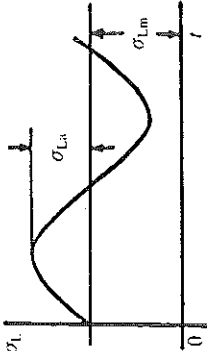
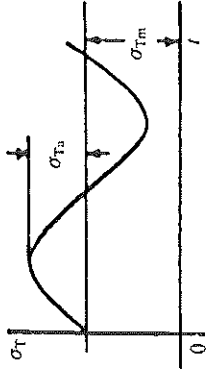
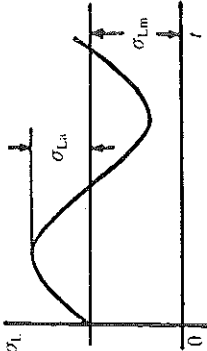
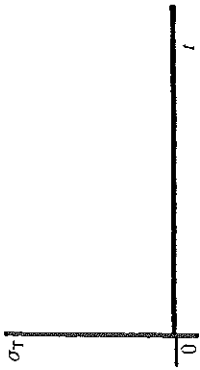
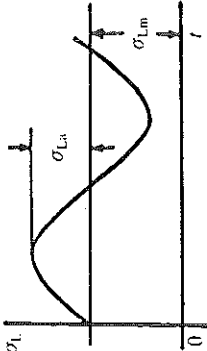
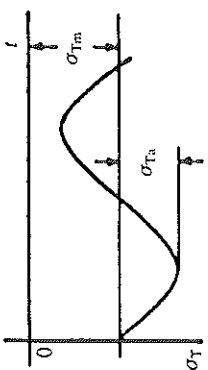
$$\sigma_L = 1.49\sigma_{y0} - 0.32\sigma_{x0} \quad (4)$$

$$\sigma_T = -0.32\sigma_{y0} + 1.49\sigma_{x0} \quad (5)$$

Table 1 Mechanical properties and chemical composition of the materials

Chemical composition (%)							
	C	Si	Mn	P	S	Ni	Cr
WT60	0.09	0.16	1.01	0.014	0.005	—	0.01
SUS304	0.06	0.57	1.00	0.027	0.006	8.47	18.16
Mechanical properties							
	Yield strength (MPa)		Tensile strength (MPa)		Elongation (%)		
WT60	539		647		20		
SUS304	284		628		60		

Table 2 Biaxial stress conditions for the corrosion fatigue tests

λ ($=\sigma_T/\sigma_L$)	Biaxial stress conditions	Stress in y direction σ_L	Stress in x direction σ_T
1	$\sigma_{Tm}/\sigma_{Lm} = 1$ $\sigma_{Ta}/\sigma_{La} = 1$ $\phi = 0$		
0	$\sigma_{Tm}/\sigma_{Lm} = 0$ $\sigma_{Ta}/\sigma_{La} = 0$ $\phi = 0$		
-1	$\sigma_{Tm}/\sigma_{Lm} = -1$ $\sigma_{Ta}/\sigma_{La} = -1$ $\phi = \pi$		

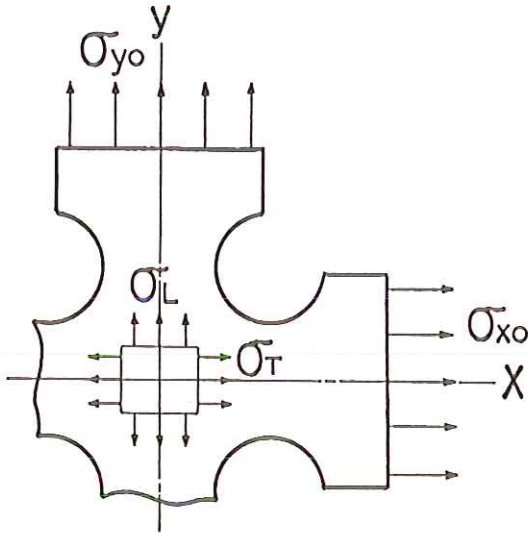


Fig 2 Stress state at the centre of a cruciform specimen without a crack

These components correspond to the uniform biaxial stresses in the y and x directions for a crack in an infinite plate, as shown in Fig. 2. Therefore, the biaxial stress ratio, λ , can be defined approximately as follows

$$\lambda = \sigma_T / \sigma_L = \Delta\sigma_T / \Delta\sigma_L \quad (6)$$

In the biaxial fatigue tests, the stress ranges $\Delta\sigma_L$ and $\Delta\sigma_T$ calculated from equations (4) and (5) were controlled and kept constant and the stress ratio R_K defined as K_{Imin}/K_{Imax} was also kept constant.

In the corrosion fatigue tests, three kinds of biaxial stress conditions were selected, which corresponded to biaxial stress ratios $\lambda = 1, 0, -1$, as shown in Table 2.

Environment and experimental conditions

In the corrosion fatigue tests, a 3.5 per cent NaCl solution was used to simulate marine environments and an acrylic chamber with a volume of 180 cc was used as shown in Fig. 3. The flow rate was about 250 cm²/hour of fresh seawater. The specimen was covered by a silicon rubber coating over all the surface except for the region where the crack grew.

In the corrosion fatigue tests of WT60, three kinds of potential conditions were employed: a free corrosion, an over-cathodic potential and an anodic potential, using a potentiostat, a Pt counter electrode, and an Ag/AgCl reference electrode, as shown in Fig. 3. The free corrosion potential was $E = -0.6$ V (Ag/AgCl), the over cathodic potential was $E = -1.2$ V (Ag/AgCl), and the anodic potential was $E = -0.4$ V (Ag/AgCl). These conditions were

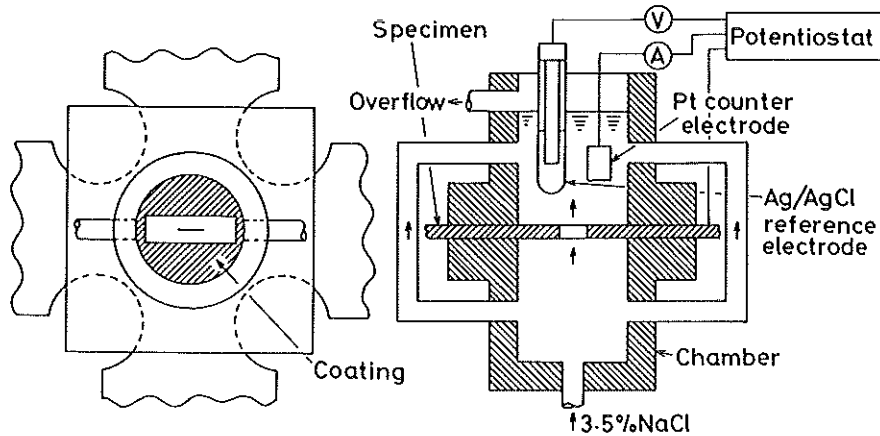


Fig 3 Schematic of the corrosion chamber and potentiostat

employed to realize different corrosion fatigue damage processes such as hydrogen embrittlement and corrosion dissolution. In the corrosion fatigue tests of SUS304, only a free corrosion condition was employed. The stress ratio R_K was 0.1 and the loading frequency was either 0.5 Hz or 7 Hz. The crack half length was measured by a travelling microscope over the range 4 to 17 mm.

All the experimental conditions are shown in Table 3. The in-air biaxial fatigue crack growth data for the same materials are reported in a previous paper (9). The stress levels $\sigma_{Lmax}/\sigma_{ys}$ (i.e., the ratio of maximum stress perpendicular to a crack to the uniaxial yield strength of the material) employed in this study for WT60 were relatively low and for which no effect of biaxial stresses on fatigue crack growth in air has been noted. The stress level for SUS304 was relatively high and at values where an effect of biaxial stresses has been noted in air.

Table 3 Experimental conditions

Material	Potential E(Ag/AgCl)	λ (σ_T/σ_L)	$\sigma_{Lmax}/\sigma_{ys}$	Crack length a	Frequency f	R_K
WT 60	-0.6 V	1	0.283	4 ~ 17 mm	0.5 and 7 Hz	0.1
	(Free corrosion)	-1				
	-0.4 V	1	0.242		0.5 Hz	
	(Anodic)	0				
	-1.2 V	1				
(Cathodic)	0					
		-1				
SUS 304	Free corrosion	1	0.483			
		0				
		-1				

Experimental results

Corrosion fatigue crack growth for WT60

Figure 4 shows the crack growth rate versus ΔK_I relations for WT60 in a 3.5 per cent NaCl solution for free corrosion conditions. This figure shows that the fatigue crack growth rate is accelerated by the environment at a low frequency and the acceleration becomes more significant at a low ΔK_I range (1). It is found that the data set for biaxial stresses reveal only a small difference, and the data for equi-biaxial stress, $\lambda = 1$, is accelerated slightly in the low and middle ranges of ΔK_I .

Figure 5 shows the corrosion fatigue crack growth behaviour of WT60 at over cathodic potential ($E = -1.2$ V) and anodic potential ($E = -0.4$ V). The data

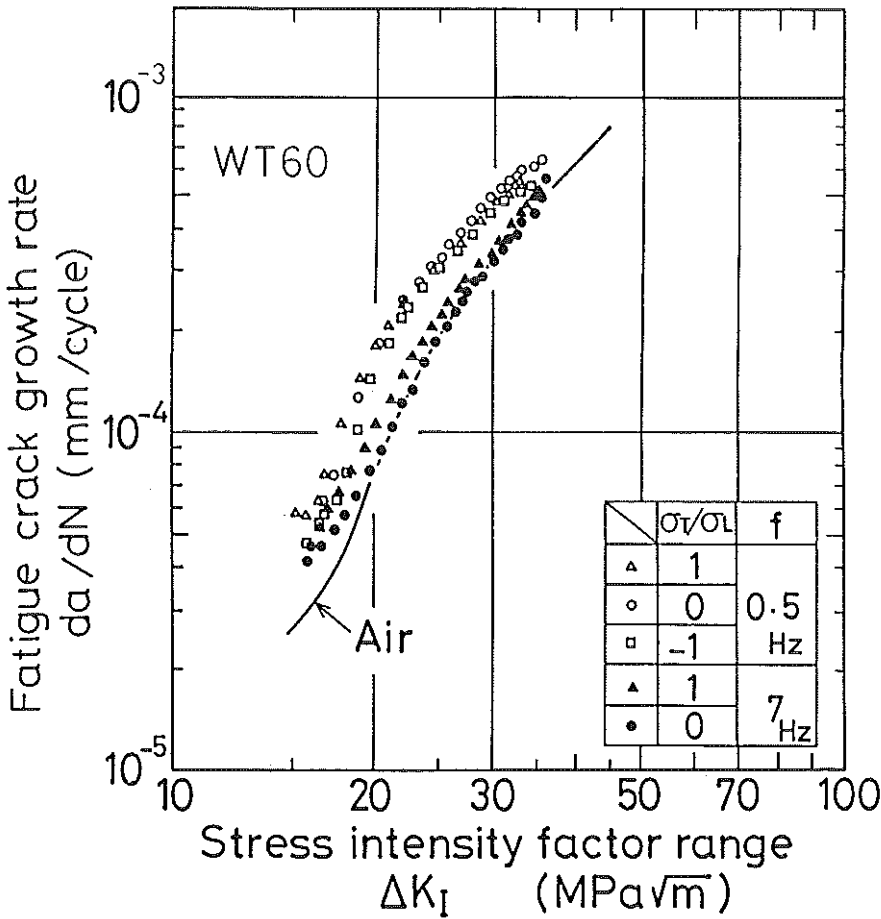


Fig 4 Corrosion fatigue crack growth in 3.5 per cent NaCl for WT60 at free corrosion at $R_K = 0.1$

at anodic potential are accelerated more than the data at free corrosion below $\Delta K_I = 18 \text{ MPa}\sqrt{\text{m}}$. No effect of biaxial stresses on the corrosion fatigue crack growth at anodic potential was observed, because the stress level is low.

The data at over-cathodic potential are accelerated significantly due to hydrogen embrittlement. A small effect of biaxial stress at over-cathodic potential was observed. In this case, it seems that the data for equi-biaxial stress, $\lambda = 1$, are decelerated. Figures 4 and 5 suggest that the order of the data for biaxial stresses is dependent on the potential.

Figure 6 shows the crack opening ratios U measured during the corrosion fatigue tests on WT60. Crack opening stress was measured in seawater by strain gauges covered by a silicon rubber coating. The crack opening ratios at three

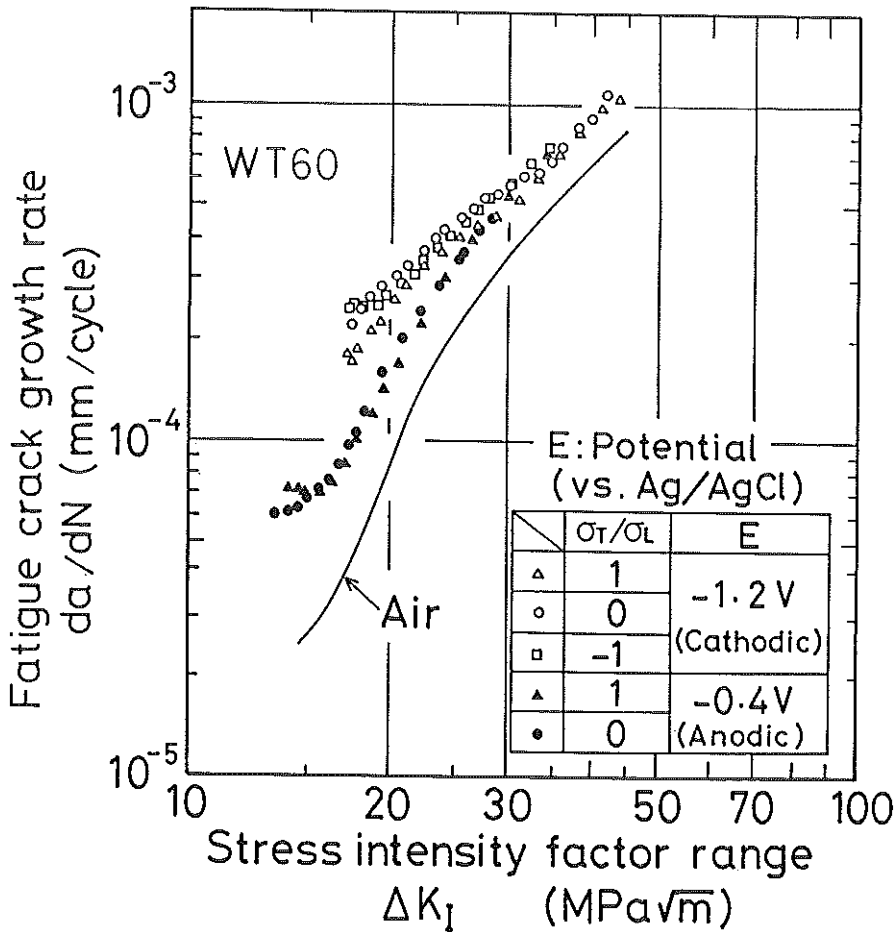


Fig 5 Corrosion fatigue crack growth for WT60 in 3.5 per cent NaCl at over-cathodic potential and anodic potential; $R_K = 0.1$ and $f = 0.5 \text{ Hz}$

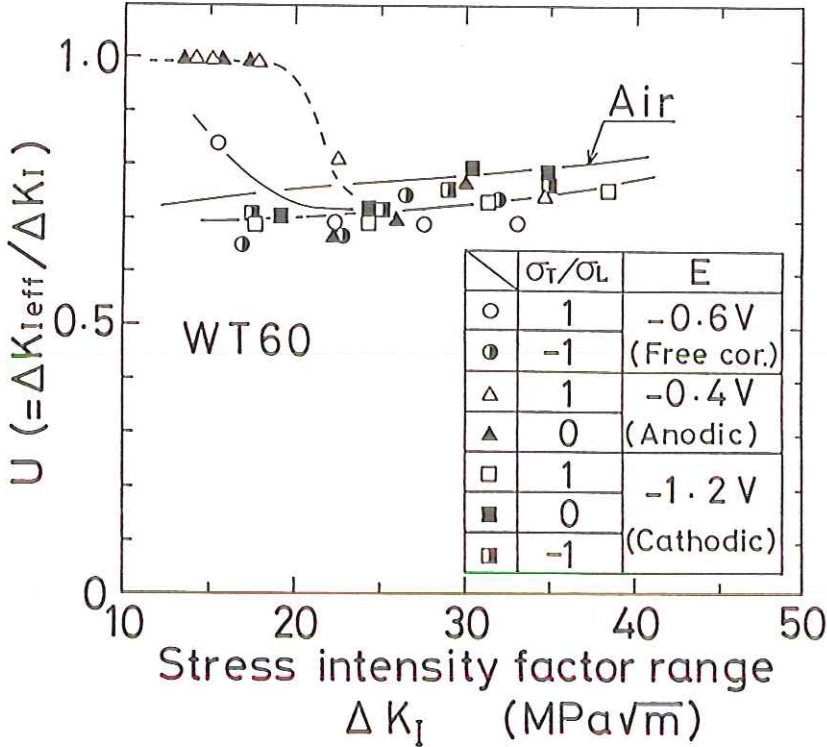


Fig 6 Crack opening ratio U for WT60 under biaxial stress in 3.5 per cent NaCl solution; $R_K = 0.1$ and $f = 0.5$ Hz

potential conditions coincide with each other at $\Delta K_I > 25$ MPa \sqrt{m} . But the crack opening ratio for an anodic potential increases below 25 MPa \sqrt{m} due to significant corrosion dissolution so that da/dN at anodic potential is accelerated at low ΔK_I ranges. No effect of biaxial stress on the crack opening ratio was observed.

Corrosion fatigue crack growth for SUS304

Figure 7 shows the corrosion fatigue crack growth properties for the stainless steel at a free corrosion condition. In this case a significant effect of biaxial stress is recorded because the stress level is relatively high; an effect of biaxial stress also appeared in air (15) as shown in Fig. 7. This figure shows that the fatigue crack growth rate in NaCl solution for uniaxial stress is fastest; however, in air it is the shear stress data which are most accelerated. Thus it depends on the environment how the effect of biaxial stress on fatigue crack growth manifests itself. This suggests that fatigue crack growth under biaxial stresses

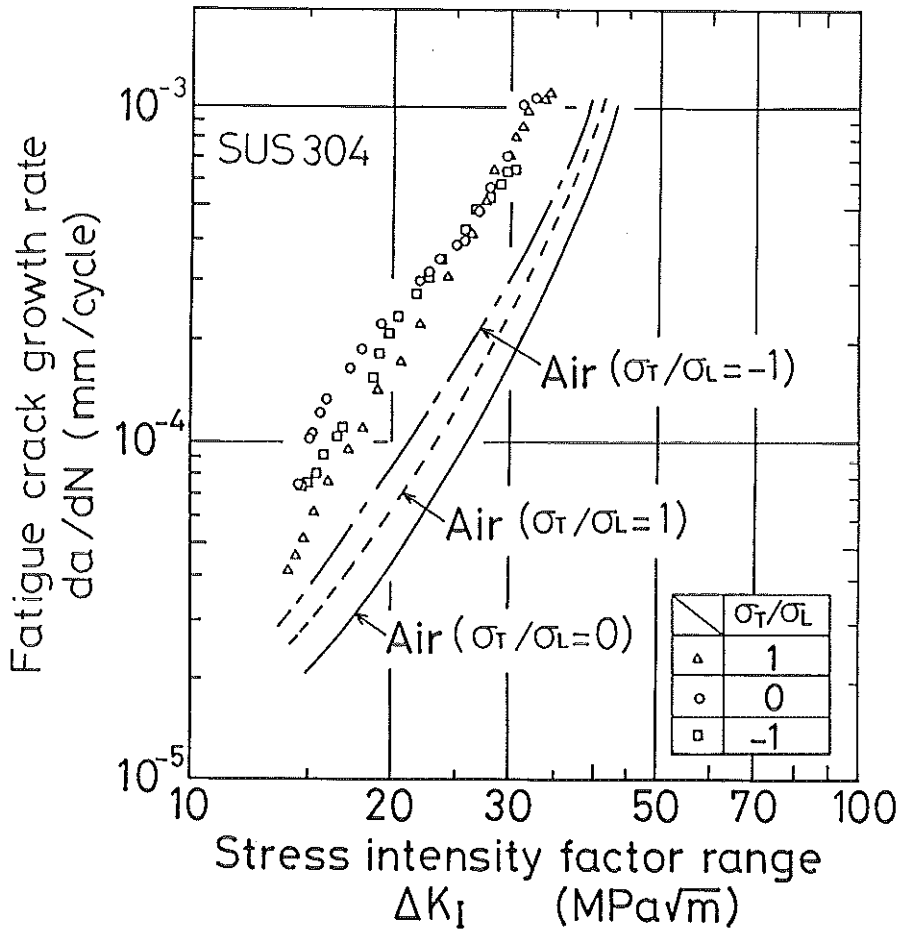


Fig 7 Corrosion fatigue crack growth for SUS304 at free corrosion in 3.5 per cent NaCl; $R_K = 0.1$ and $f = 0.5$ Hz

cannot be simply correlated by parameters, such as the crack tip plastic zone size, and certainly not by LEFM analyses, when environmental conditions are important.

Effect of corrosive environments

Figure 8 presents the ratio of the fatigue crack growth rate in a corrosive environment to that in air for all tests as a function of ΔK_I . The corrosion fatigue crack growth rates for the high tensile steel (WT60) are accelerated in the order of over-cathodic potential, free corrosion, and anodic potential, although the

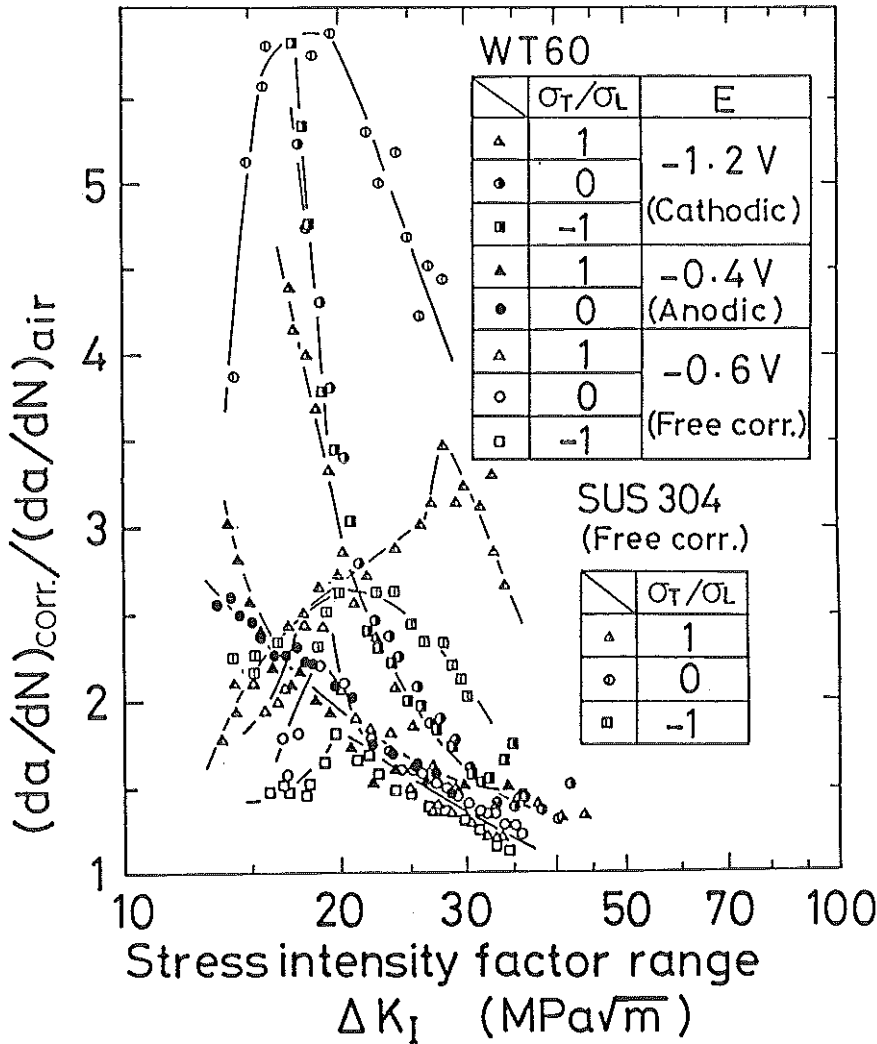


Fig 8 The ratio of crack growth rate in 3.5 per cent NaCl solution and in air versus stress intensity factor range ΔK_I ; $R_K = 0.1$ and $f = 0.5$ Hz

order is also affected by the level of ΔK_I . Those for SUS304 are accelerated more than WT60. The maximum ratio reaches 6.0. The acceleration is significant at a low ΔK_I range. It is noteworthy that the ratio of growth rates increases with decrease of ΔK_I at the anodic condition and the over-cathodic condition. However, the ratio has a peak value for the free corrosion condition. Similar results have been reported on corrosion fatigue crack growth for various materials under uniaxial loading in seawater (11)(12).

Discussion

It is to be expected that the effect of biaxial stresses on the fatigue crack growth in NaCl solution will be different from that in air because of fatigue-environment interactions. The effect of biaxial stress on the corrosion fatigue crack growth is discussed below and is compared with the effect in air.

A parameter to measure this effect is the ratio of the maximum value of da/dN to the minimum value of da/dN at various biaxial stresses and specific values of ΔK_I . Figure 9 shows the ratio of $(da/dN)_{\max}/(da/dN)_{\min}$, both in NaCl solution and in air (15), versus half crack length. It will be noted that in these tests the applied loads are constant, and so crack length corresponds approximately to ΔK_I^2 . Should no effect of biaxial stress appear, then LEFM can be applied in the case when the ratio equals 1.0. For cases where the ratio becomes greater than 1.5, then a significant effect of biaxial stress occurs and LEFM is not applicable.

Figure 9(a) shows that the ratio of the fatigue crack growth rates in NaCl solutions increases with a decrease of crack length and attains a peak value. Figure 9(b) shows that the max/min speed ratio in air increases monotonically with decrease of crack length. These figures suggest that a more significant effect of biaxial stress on fatigue crack growth appears when a crack is small. Therefore, it is to be expected that the fatigue crack growth rate for a short or small crack will be affected significantly by biaxial stresses. The fact that the ratio $(da/dN)_{\max}/(da/dN)_{\min}$ has a peak value in Fig. 9(a) corresponds to the phenomenon that corrosion fatigue crack growth at a free corrosion condition is accelerated significantly at $\Delta K_I = 20\text{--}30 \text{ MPa}\sqrt{\text{m}}$, as shown in Fig. 8. This means that a more significant effect of biaxial stress will appear where the fatigue crack growth rate is accelerated significantly in a corrosive environment.

Figure 10 and Table 4 display all the biaxial fatigue crack growth tests for WT60 and SUS304, both in air and in NaCl solution. The data in air are partly reported in a previous paper (9) where a comprehensive study on fatigue crack growth under biaxial stresses was reported. Focussing attention on crack length and applied stress level, the critical region where the effect of biaxial stresses appears is best clarified after a definition of the effect as given in Fig. 9. This figure indicates that LEFM is not applicable when the stress level reaches $\approx 0.4\text{--}0.6 \sigma_{ys}$ for both materials, and that the critical region where the effect of biaxial stress appears depends on crack length. Therefore, if a crack is small, the effect of biaxial stress should appear to be significant even if the stress level is not so high. This figure is also important in understanding the various conflicting conclusions on the effect of biaxial stress on fatigue crack growth as reported by several researchers (2)–(10).

In this figure, the experimental conditions of corrosion fatigue tests previously shown are included. The stress levels of the tests on WT60 at three potential conditions were relatively low so that a significant effect of biaxial stress could not be observed. However, a significant effect appeared in the corrosion fatigue tests on SUS304 at free corrosion because the stress level was

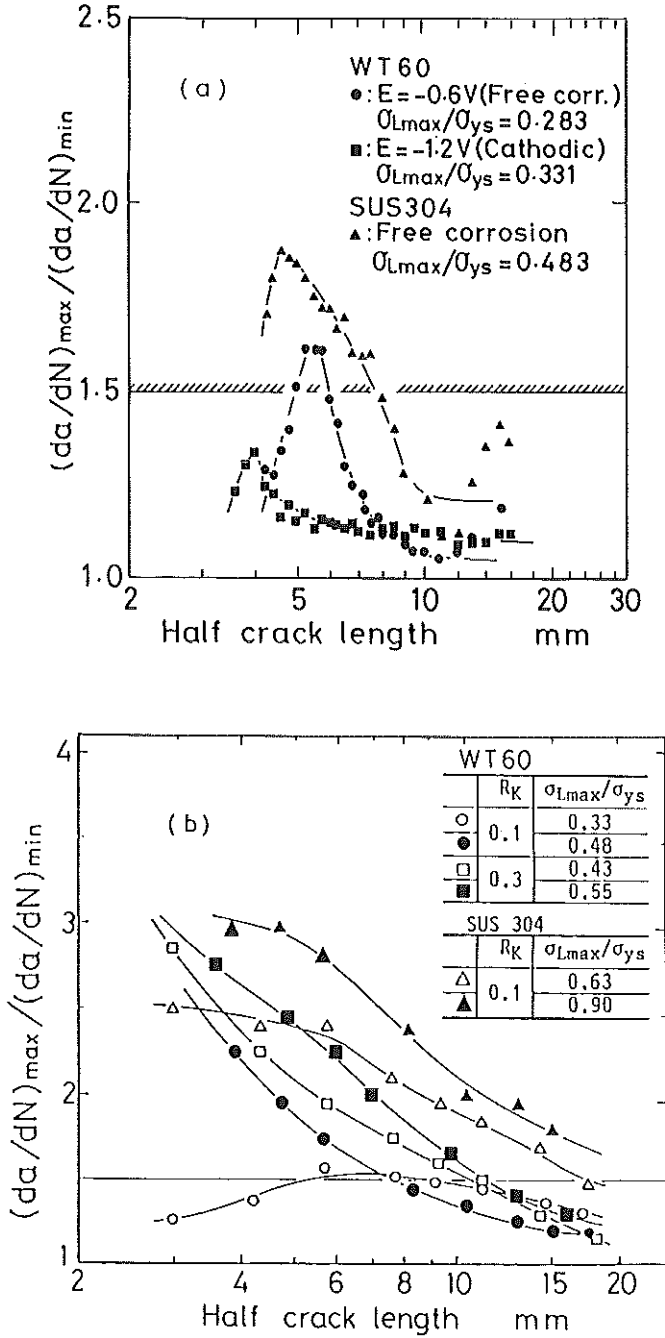


Fig 9 Effect of biaxial stress on fatigue crack growth in SUS304 and WT60: (a) in 3.5 per cent NaCl solution, $R_K = 0.1$ and $f = 0.5$ Hz; (b) in air; $R_K = 0.1$ and 0.3

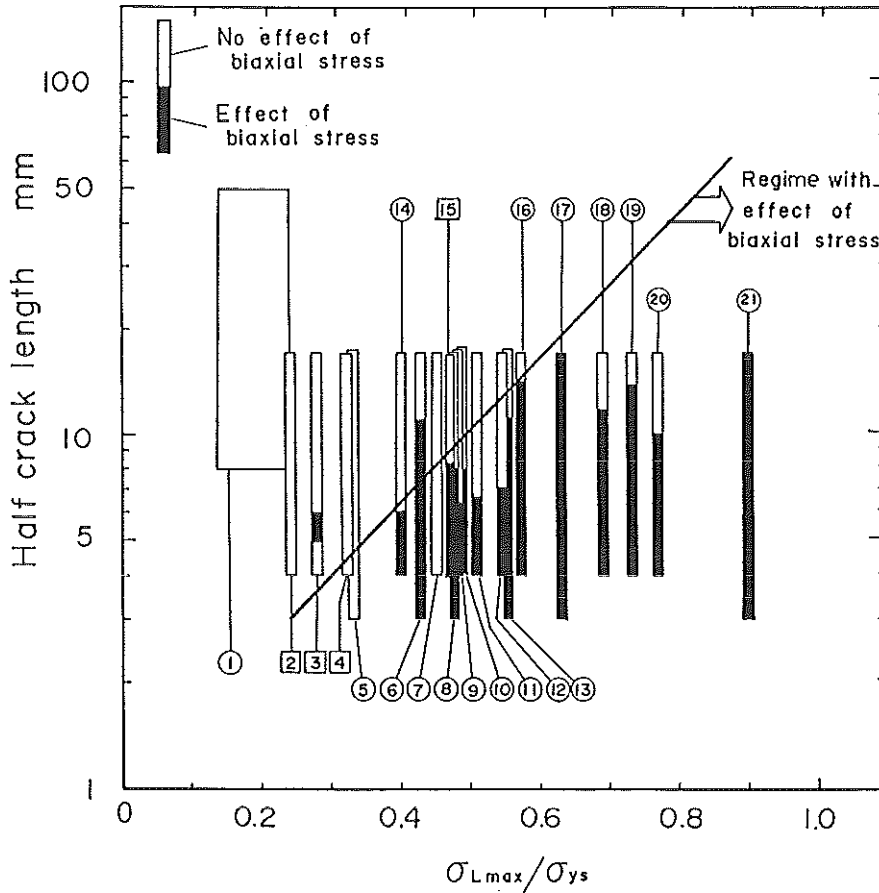


Fig 10 Experimental conditions for various biaxial fatigue tests (see Table 4)

relatively high where the effect of biaxial stresses also appears significant in in-air tests.

The effect of biaxial stress on fatigue crack growth properties is different for the various biaxial stress conditions. The order of the data set for biaxial stresses is also quite different between in-air and in-seawater, as shown in Fig. 7, and also different between cathodic potential and free corrosion, as shown in Figs 4 and 5. Moreover, a previous paper (9) pointed out that the order of a data set for biaxial stresses in air is different between materials. Therefore, the effect of biaxial stresses on fatigue crack growth depends on the material and the environment. This means that fatigue crack growth under biaxial stresses cannot be explained by the plastic zone size or crack opening displacement. It seems to be very difficult to evaluate quantitatively the effect of biaxial stresses on fatigue crack growth in various environments at present

Table 4 Key to the stress ratio values and environments for the data given in Fig. 10

<i>WELTEN 60</i>			<i>SUS 304</i>		
<i>No.</i>	R_K	<i>Environment</i>	<i>No.</i>	R_K	<i>Environment</i>
1	0.1, 0.3	In air	14	0.1	In air
2	0.1	Corrosion $E = -0.4$ V (anodic)	15	0.1	Corrosion (free corr.)
3	0.1	Corrosion $E = -0.6$ V (free corr.)	16	0.1	In air
4	0.1	Corrosion $E = -1.2$ V (cathodic)	17	0.1	In air
5	0.1	In air	18	0.1	In air
6	0.3	In air	19	0.2	In air
7	0	In air	20	0.1	In air
8	0.1	In air	21	0.1	In air
9	0.4	In air			
10	0.1	In air			
11	0.3	In air			
12	0.2	In air			
13	0.3	In air			

(15). Only a few data on corrosion fatigue crack growth are reported in this paper and a comprehensive study on this problem is needed. It is expected that a significant effect of biaxial stresses will occur in corrosive environments.

Conclusions

Corrosion fatigue tests of a high tensile steel and a stainless steel in a 3.5 per cent NaCl solution were carried out under various in-plane biaxial stress conditions and the effects of biaxial stresses on the corrosion fatigue crack growth were investigated and compared with those in air. The main results are as follows.

- (1) The effects of biaxial stresses on corrosion fatigue crack growth appear in a similar regime as effects of biaxial stresses in air. Only a small effect of biaxial stresses in NaCl solution appears where no effect of biaxial stresses was observed in air.
- (2) Where the fatigue crack growth rate is accelerated significantly by a corrosive environment in a uniaxial test, it seems that the effect of biaxial stresses is also significant.
- (3) It is found that the order of a data set for biaxial stress conditions in NaCl solution is different from that in air and also differs between a free corrosion condition and a cathodic condition. It depends on the material and the environment how the effect of biaxial stresses manifests itself on fatigue crack growth.
- (4) It is expected that a significant and particular effect of biaxial stresses on corrosion fatigue growth will appear in the region where a crack is small

and the stress level is correspondingly high. A more comprehensive study on corrosion fatigue crack growth under biaxial stresses for short cracks subjected to high cyclic stresses is urgently required.

References

- (1) JASKE, C. E., PAYER, J. H., and BALIENT, V. S. (1981) *Corrosion Fatigue of Metals in Marine Environments*, Battelle Press, Springer-Verlag, Berlin.
- (2) KIBLER, J. J. and ROBERTS, R. (1970) The effect of biaxial stresses on fatigue and fracture, *J. Engng Ind. Trans ASME, Ser. B*, **92**, 727-734.
- (3) MILLER, K. J. and HOPPER, C. D. (1977) Fatigue crack propagation in biaxial stress fields. *J. Strain Analysis*, **121**, 23-28.
- (4) MILLER, K. J. (1977) Fatigue under complex stress, *Met. Sci.*, **11**, 432-438.
- (5) LIU, A. F., ALLISON, J. E., DITTNER, D. F., and YAMANE, J. R. (1979) *Effect of biaxial stresses on crack growth*, *ASTM STP 677*, pp. 5-22.
- (6) TANAKA, K., HOSHIDE, T., YAMADA, A., and TAIRA, S. (1979) Fatigue crack propagation in biaxial stress fields, *Fatigue Engng Mater. Structures*, **2**, 181-194.
- (7) HOSHIDE, T., TANAKA, K., and YAMADA, A. (1981) Stress-ratio effect of fatigue crack propagation in a biaxial stress field, *Fatigue Engng Mater. Structures*, **4**, 355-366.
- (8) KITAGAWA, H., YUUKI, R., and TOHGO, K. (1979) A fracture mechanics approach to high-cycle fatigue crack growth under in-plane biaxial loads, *Fatigue Engng Mater. Structures*, **2**, 195-206.
- (9) KITAGAWA, H., YUUKI, R., and TOHGO, K. (1985) ΔK -dependency of fatigue growth of single and mixed mode cracks under biaxial stress, *ASTM STP 853*, pp. 164-183.
- (10) BROWN, M. W. and MILLER, K. J. (1985) *Mode I fatigue crack growth under biaxial stress at room and elevated temperature*, *ASTM STP 853*, pp. 135-152.
- (11) KOMAI, K., MINOSHIMA, K., and YAMAMOTO, K. (1984) Corrosion fatigue crack growth in high tensile strength steel under cathodic overprotection, *J. Soc. Mater. Sci.* (in Japanese), 33-374, 1407-1413.
- (12) BARDALL, E., SØNDENFOR, J. M., and GARTLAND, P. O. (1980) Slow corrosion fatigue crack growth in a structural steel in artificial seawater at different potentials, crack depths and loading frequencies, *Proc. European Offshore Research Seminar*, Vol. I, p. 16.
- (13) MILLER, K. J. and KFOURI, A. P. (1974) An elastic-plastic finite element analysis of crack tip fields under biaxial loading conditions, *Int. J. Fracture*, **10**, 393-404.
- (14) ADAMS, N. J. I. (1973) Some comments on the effect of biaxial stress on fatigue crack growth and fracture, *Engng Fracture Mech.*, **5**, 983.
- (15) YUUKI, R., KITAGAWA, H., TOHGO, K., and TANABE, M. (1985) Effect of biaxial stresses and its factors on fatigue crack growth properties, *Trans. Jap. Soc. mech. Engrs* (in Japanese), 51-469, 2057-2066.